

Recognition of Fatigue Driving Based on Steering Operation Using Wearable Smart Watch



Dihua Sun, Yong Huang, Min Zhao, Dong Chen and Weijian Han

Abstract Given the growing popularity of wearable smart watch with the capability to detect human hand movements, this paper studies the potential to recognize fatigue driving based on steering operation by using a wearable smart watch. The sensor data used includes acceleration and angular velocity data related to drivers' operation behavior. We analyze the sensors' data features of smart watch under drivers' fatigue and normal states, and select 13 principal characteristic parameters by using the method of principal component analysis (PCA). Then the recognition model of fatigue driving based on support vector machine (SVM) is established. The results show that the proposed method recognizes the drivers' fatigue or normal state more effectively than other methods and its accuracy can reach 83.29%.

Keywords Fatigue driving · Operation behavior · Smart watch · Support vector machine

1 Introduction

Driving is a hard task that drivers always have to watch road and make right operation decisions on time. They are subsequently prone to fatigue after driving for a long time and the ability to control the vehicle will be weakening. Studies show more than 35% of serious traffic accidents are caused by fatigue driving [1]. Therefore, it is necessary to recognize driver's fatigue state effectively by some advanced methods for reducing traffic accidents caused by fatigue driving.

In the existing literature, researchers have made full use of many factors to recognize fatigue driving, which include drivers' facial expression [2, 3], physiological

D. Sun · Y. Huang (✉) · M. Zhao · D. Chen

Key Laboratory of Dependable Service Computing in Cyber Physical Society of Ministry of Education, Chongqing University, Chongqing 400044, China
e-mail: huangyong2016@cqu.edu.cn

College of Automation, Chongqing University, Chongqing 400044, China

W. Han

College of Automotive Engineering, Chongqing University, Chongqing 400044, China

© Springer Nature Singapore Pte Ltd. 2020

W. Wang et al. (eds.), *Green, Smart and Connected Transportation Systems*,
Lecture Notes in Electrical Engineering 617,
https://doi.org/10.1007/978-981-15-0644-4_18

characteristics [4, 5] and operation behavior [6–8]. Facial expression-based methods are recognized by analyzing changes of facial expression, such as yawning and blinking. Nevertheless, many external factors, such as illumination and head position change, have an important impact on recognition accuracy. Physiological characteristics-based methods are high in accuracy, but majority of them need to place many sensors on drivers' body for data acquisition, which often make the drivers uncomfortable. Operation behavior-based methods recognize drivers' fatigue state by analyzing operation changes of steering wheel and vehicle status, such as the standard deviation of the steering wheel angle and lane departure, which can avoid the shortcomings of the previous methods and have become an important part of fatigue driving recognition research. Wei et al. [9] chose the lateral position and steering wheel angle as the input data of neural network and trained it by BP algorithm. His experiment results showed that this method is effective to recognize drivers' fatigue level. McDonald et al. [10] analyzed the characteristics of drivers' steering data and established a fatigue driving recognition model based on random forest algorithm, which had a higher classification accuracy.

However, the existing majority of operation behavior based methods are to collect the related data by installing various sensors on steering wheel and vehicle, which are too complicated to be practical. In recent years, wearable smart watch with a variety of sensors, have been widely popularized and used to detect human body motion in some research works. Mannini et al. [11] utilized wrist-worn accelerometer to collect wrist and ankle motion data and classified behavior into four classes: sedentariness, cycling, ambulation and other, and the results showed high classification accuracy for ankle data (95.0%) and wrist data (84.7%). Shoaib et al. [12] used wrist-worn motion sensors to recognize hand gestures and it can accurately detect 13 activities. These researches have showed that motion sensors in wearable devices can accurately reflect human's behavior.

According to the above analysis, this paper studies a fatigue driving recognition method based on steering operation by using a smart watch. Thirteen characteristic parameters are extracted from smart watch's sensors based on driving simulation experiment and the fatigue driving recognition model is established based on support vector machine. The test results prove that we can use smart watch to recognize the drivers' fatigue or normal state. This work uses no other external sensors, bringing about a low cost, user-friendly and simple recognition system.

2 Experiments of Data Acquisition

2.1 Experimental Design

Driving experiments are carried out on the Multi-Vehicle Cooperative Simulation Platform, as shown in Fig. 1, in Key Laboratory of Dependable Service Computing in Cyber Physical Society Ministry of Education (CPS-DSC), Chongqing University.

Fig. 1 Driving simulation platform

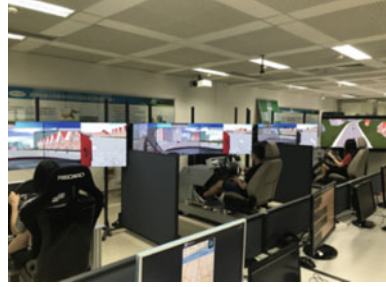


Fig. 2 Simulation scene



The simulation road is a 100 km long highway of part of the Yuxiang highway located between Chongqing and Hunan province, with two lane in one direction. The smart watch used in the experiment is TicWatch, and it has acceleration sensor, gyroscope sensor, gravity sensor and geomagnetic sensor. Ten participants (six men and four women have an average of 3.5 years driving experience) aged between 24 and 30 years old took part in the experiment from 13:00 pm to 14:30 pm, who are most likely to be fatigued in this period. They have had a good command of the driving scene before the experiment and are asked to wear smart watch for driving during experiments, as shown in Fig. 2. Besides, all participants are required to reduce the lane change and keep the speed of 80 ± 10 km/h when the vehicle is moving.

2.2 Data Acquisition

In the process of the whole experiments, three types of data are recorded synchronously, including:

- (1) The data values of smart watch's acceleration sensor, gyroscope sensor, gravity sensor, and geomagnetic sensor are recorded at the frequency of 10 Hz;
- (2) Video of the drivers' facial expression;
- (3) The drivers' self-evaluation of fatigue or normal state every ten minutes according to the Karolinska Sleepiness Scale (KSS) [13].

The video of drivers' facial expression and the drivers' self-evaluation are used to judge the drivers' states. There may be a deviation between drivers' self-evaluation and actual fatigue degree. In order to improve the accuracy of the fatigue degree, three trained experts evaluate the drivers' states according to the video in different periods and modify the KSS score of the drivers' self-evaluation. In this study, driving state of the driver is classified into two classes. If KSS score ≤ 3 , the driver is under normal state and is under fatigue state while KSS score ≥ 7 [14].

3 Methods

3.1 Method Design

In order to establish the fatigue recognition model and recognize the drivers' states effectively, there are several key steps to do, including driving simulation experiment, coordinate system transformation, characteristic extraction (principal component analysis), training and testing recognition model of fatigue driving based on SVM, as shown in Fig. 3.

3.2 Data Processing

The motion sensors of smart watch use a standard 3-axis device coordinate system to express data values. The X-axis is horizontal and points to the right, the Y-axis

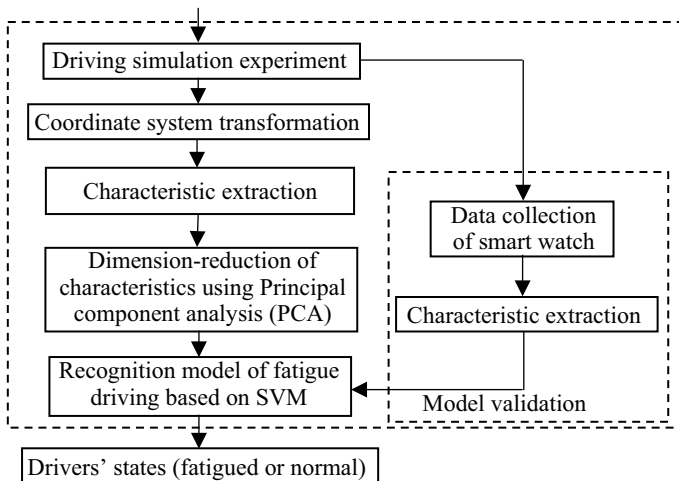


Fig. 3 Flow diagram of fatigue recognition model

Fig. 4 Device coordinate system

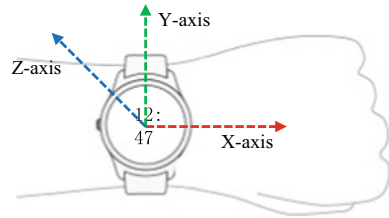
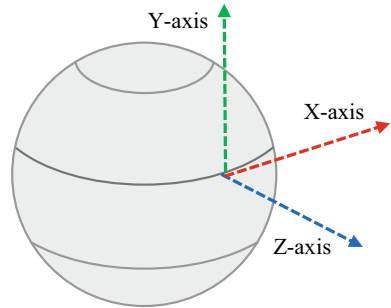


Fig. 5 World's coordinate system



is vertical and points up, and the Z-axis points toward the outside of the screen, as shown in Fig. 4. The attitude of smart watch will be constantly changing in the course of data acquisition and the data values of gravitational acceleration on the three axes will be changing too. Therefore, it is critical to eliminate the effect of gravitational acceleration on the data values of acceleration sensor.

We transform the data values of acceleration sensor from device coordinate system to the world's coordinate system whose X-axis is tangential to the ground and roughly points East, Y-axis is tangential to the ground and points towards the magnetic North Pole, and Z-axis points towards the sky vertically (as shown in Fig. 5):

$$\begin{bmatrix} x' \\ y' \\ z' \end{bmatrix} = R \cdot \begin{bmatrix} x \\ y \\ z \end{bmatrix} = \begin{bmatrix} R_1 & R_2 & R_3 \\ R_4 & R_5 & R_6 \\ R_7 & R_8 & R_9 \end{bmatrix} \cdot \begin{bmatrix} x \\ y \\ z \end{bmatrix} \tag{1}$$

where x, y, z express the values of acceleration sensor in the device coordinate system and x', y', z' are in the world's coordinate system, R expresses a 3×3 row-major matrix that can be computed with the values of gravity sensor and geomagnetic sensor. When the values of acceleration sensor in the world's coordinate system is got, only the value of Z-axis contains the constant of gravitational acceleration and we can eliminate it directly.

3.3 Characteristics Extraction

3.3.1 Analysis and Extraction of Characteristics

The data of drivers' steering operation includes rotation acceleration and angular velocity of steering wheel that we can get from smart watch's motion sensors. Take rotation acceleration for an example, Figs. 6 and 7 are the data change graphs of rotation acceleration (relative to the world's coordinate system) under normal driving and fatigue driving respectively. It can be seen from the graphs that the steering wheel is corrected frequently and the acceleration amplitude of correction is small under normal driving. However, the correction frequency decreases and the correction

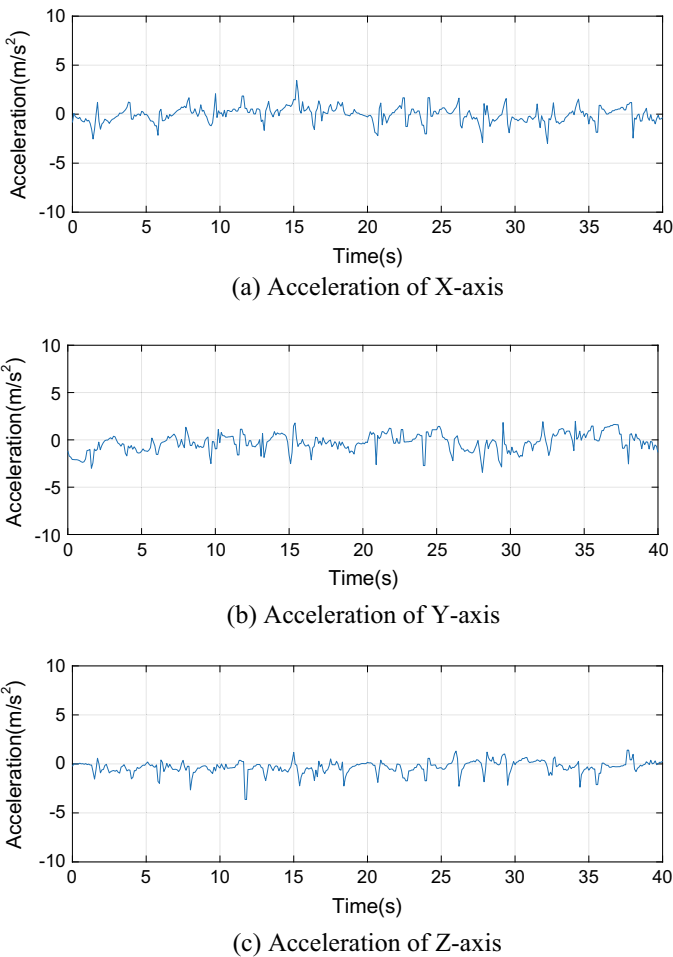


Fig. 6 Acceleration under normal driving

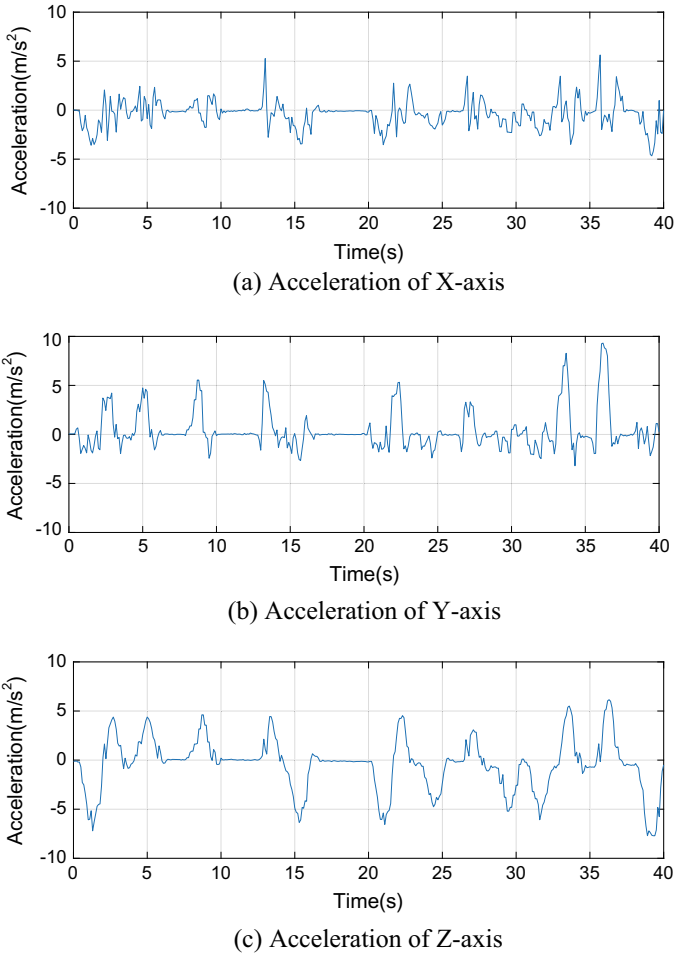


Fig. 7 Acceleration under fatigue driving

amplitude of acceleration becomes larger under fatigue driving. To summarize, the correction frequency and amplitude are different under two different driving states.

In order to describe different driving states more accurately, a series of statistical characteristic parameters are defined as listed in Table 1. Taking the duration of fatigue operation and real-time of the recognition model into account, the time window in data series is ten seconds when extracting each characteristic parameter. PLAA and PSAA mean the percentage of the acceleration amplitude that is greater or less than a threshold of the time window:

$$PLAA = \frac{\sum_{i=1}^n LA_i}{n} \times 100\%, LA_i = \begin{cases} 1, & \text{if } A_i \geq \text{mean_}Q2(AF) \\ 0, & \text{if } A_i < \text{mean_}Q2(AF) \end{cases} \quad (2)$$

Table 1 Characteristic parameters and meaning

Characteristic parameters	Meaning
MA	Mean acceleration of steering wheel (X-axis/Y-axis/Z-axis)
SDA	Standard deviation of steering wheel acceleration (X-axis/Y-axis/Z-axis)
RMSA	Root mean square of steering wheel acceleration
PLAA	Percentage of large acceleration amplitude
PSAA	Percentage of small acceleration amplitude
MAV	Mean angular velocity of steering wheel (X-axis/Y-axis/Z-axis)
SDAV	Standard deviation of steering wheel angular velocity (X-axis/Y-axis/Z-axis)
RMSAV	Root mean square of steering wheel angular velocity
PLAVA	Percentage of large angular velocity amplitude
PSAVA	Percentage of small angular velocity amplitude

$$PSAA = \frac{\sum_{i=1}^n SA_i}{n} \times 100\%, SA_i = \begin{cases} 1, & \text{if } A_i < \text{mean_}Q2(AN) \\ 0, & \text{if } A_i \geq \text{mean_}Q2(AN) \end{cases} \quad (3)$$

where n is the data number of the time window, A_i expresses the value of synthetic acceleration in data series, $\text{mean_}Q2(AF)$ is the mean value of synthetic acceleration that is greater than median in data series under fatigue state, and $\text{mean_}Q2(AN)$ is the mean value of synthetic acceleration that is greater than median in data series under normal state. PLAVA and PSAVA mean the percentage of the angular velocity amplitude that is greater or less than a threshold of the time window:

$$PLAVA = \frac{\sum_{i=1}^n LV_i}{n} \times 100\%, LV_i = \begin{cases} 1, & \text{if } AV_i \geq \text{mean_}Q2(AVF) \\ 0, & \text{if } AV_i < \text{mean_}Q2(AVF) \end{cases} \quad (4)$$

$$PSAVA = \frac{\sum_{i=1}^n SV_i}{n} \times 100\%, SV_i = \begin{cases} 1, & \text{if } AV_i < \text{mean_}Q2(AVN) \\ 0, & \text{if } AV_i \geq \text{mean_}Q2(AVN) \end{cases} \quad (5)$$

where n is the data number of the time window, AV_i expresses the value of synthetic angular velocity in data series, $\text{mean_}Q2(AVF)$ is the mean value of synthetic angular velocity that is greater than median in data series under fatigue state, and $\text{mean_}Q2(AVN)$ is the mean value of synthetic angular velocity that is greater than median in data series under normal state. We got a total of 953 samples and randomly selected 600 samples are used to train the recognition model and the other samples are used to test the model.

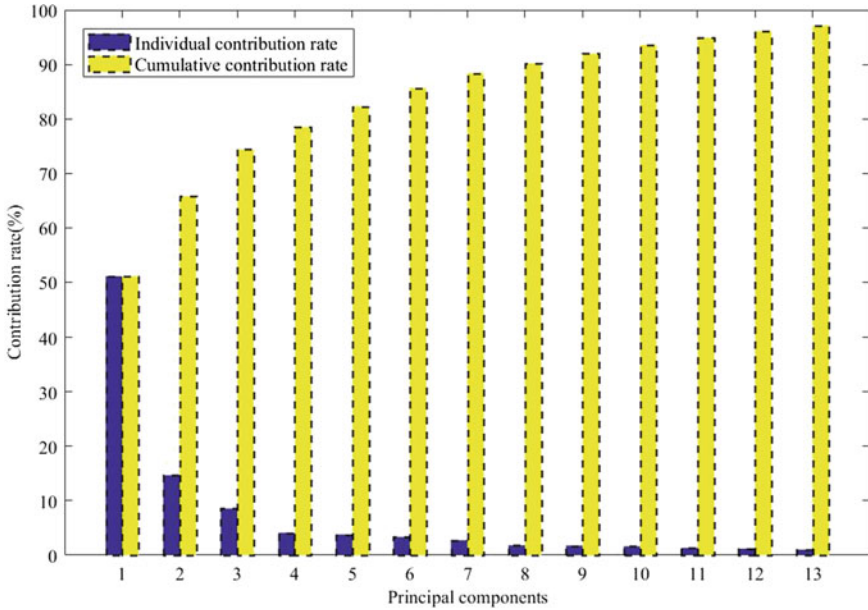


Fig. 8 Contribution rate of the principal components

3.3.2 Principal Component Analysis

We know the number of characteristic parameters is far more than ten because the coordinate system has three axes in Table 1. There may be a strong correlation among these parameters and they have a significant impact on the performance of the recognition algorithm. Thus, it is import to reduce dimensionality of these parameters consisting of some interrelated parameters, while retaining as much as possible of the variation present in them. In this paper, the normalized characteristic data is analyzed by the method of Principal Component Analysis (PCA) and the number of characteristic parameters is reduced from 18 to 13. As shown in Fig. 8, the final 13 principal component parameters are inputs of the recognition model.

3.4 Recognition Model

3.4.1 Support Vector Machine (SVM)

Since the SVM was firstly proposed in 1995 by Cortes and Vapnik [15], it had been widely used for its good classification performance. The principle of support vector machines is to find an optimal hyperplane that separates two classes and is at equal distance from the two. The margin between the optimal hyperplane and the two

classes is maximal. As shown in Fig. 9, H is an optimal hyperplane and it is at equal distance from H_1 and H_2 .

Suppose a sample set to be $\{(x_i, y_i)\}, i = 1, 2, \dots, m, x \in R^n, y_i \in \{-1, 1\}$, where there are m samples for training the SVM, R^n is the n -dimensional feature vector and y_i is the category label. When the feature vectors of samples in different classes are linearly separable, the hyperplane $\omega \cdot x + b = 0$ must satisfy the following inequalities that can separate all samples accurately:

$$y_i(\omega \cdot x_i + b) \geq 1, i = 1, 2, \dots, m \tag{6}$$

The margin can be calculated as:

$$\min_{\{x_i|y_i=1\}} \frac{\omega \cdot x_i + b}{\|\omega\|} - \max_{\{x_i|y_i=-1\}} \frac{\omega \cdot x_i + b}{\|\omega\|} = \frac{2}{\|\omega\|} \tag{7}$$

The optimal hyperplane requires the maximization of the margin, which is to mean:

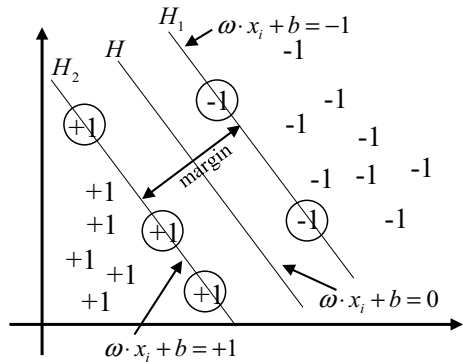
$$\max \frac{1}{2} \|\omega\|^2 = \frac{1}{2} (\omega \cdot \omega) \tag{8}$$

After using the Lagrange dual transformation, the optimal solution of the following objective function is the optimal hyperplane:

$$\begin{cases} \max \sum_{i=1}^m \alpha_i - \frac{1}{2} \sum_{i,j=1}^m \alpha_i \alpha_j y_i y_j (x_i \cdot x_j) \\ s.t. y_i [(\omega \cdot x_i) + b] - 1 \geq 0, \sum_{i=1}^m y_i \alpha_i = 0, \alpha_i \geq 0, i = 1, 2, \dots, m \end{cases} \tag{9}$$

where α_i is Lagrange multiplier of sample data i .

Fig. 9 Optimal hyperplane



When the classification problem is nonlinearly separable, the n-dimensional feature vector can be mapped into a higher dimensional space by using the mapping relationship of $z = \Phi(x)$ and the nonlinear classification problem will be linearly separable by using appropriate kernel function $k(x_i, x_j)$ in high-dimensional space. Then, the optimal solution of the following objective function is the optimal hyperplane:

$$\begin{cases} \max \sum_{i=1}^m \alpha_i - \frac{1}{2} \sum_{i,j=1}^m \alpha_i \alpha_j y_i y_j k(x_i \cdot x_j) \\ s.t. y_i [(\omega \cdot z_i) + b] - 1 \geq 0, \sum_{i=1}^m y_i \alpha_i = 0, \alpha_i \geq 0, i = 1, 2, \dots, m \end{cases} \quad (10)$$

3.4.2 Model Training

To recognize the driver’s fatigue state accurately, this paper uses SVM algorithm for fatigue recognition. Polynomial kernel and radial basis function (RBF) kernel are two popular kernels commonly used in SVM classification at present. Considering that the RBF kernel can realize nonlinear mapping and less hyper parameters can reduce the complexity of the SVM model compared to polynomial kernel, we choose RBF as the kernel for recognition model of fatigue driving. There are two parameters C and g are not known before model training, where penalty factor C expresses the tolerance of error and g in the RBF kernel has an important impact on model prediction. In order to improve the prediction performance of the model, the grid search algorithm is used to optimize the parameters C and g in this paper and the results of optimization are shown in Fig. 10. Finally, the recognition model is trained by using the two optimal parameters and randomly selected 600 samples collected from previous experiments.

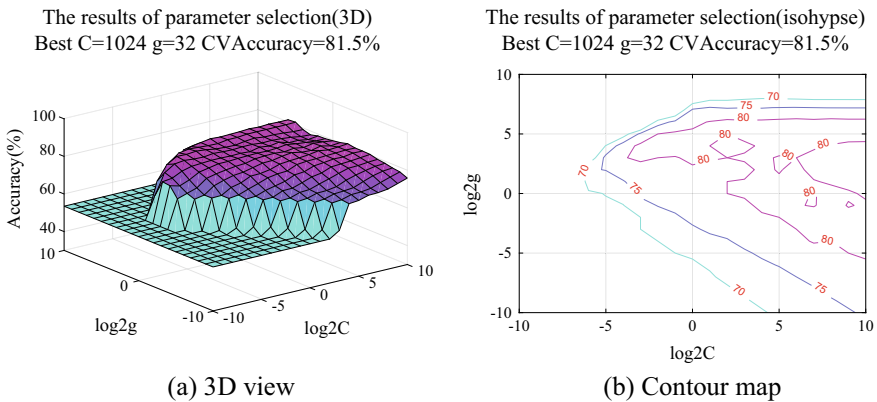


Fig. 10 Results of parameter optimization

4 Experimental Results and Discussion

After trained, the recognition model is tested with the other 353 samples, including 168 samples of normal state and 185 samples of fatigue state, and the test results are shown in Table 2. Accuracy is calculated as:

$$accuracy = (TP + TN) / T \times 100\% \tag{11}$$

where TP expresses the number of fatigue state correctly recognized as fatigue; TN expresses the number of normal state correctly recognized as normal, and T means the total test sample number of fatigue and normal state.

Table 2 shows the recognition model, which can classify the drivers' states into two classes, correctly identifies 131 samples of normal state and 163 samples of fatigue state and the accuracy of classification is 83.29%. Figure 11 shows the performance of the used model in this paper and the other related models for fatigue driving recognition. All of these models are trained and tested using the same samples with previous SVM. From Fig. 11, we can conclude that the classification accuracy of SVM used in this paper is higher than other models.

Besides, it is noticed that 37 of 168 normal state samples are incorrectly classified and misjudgment is up to 22.02% in Table 2. The reason for the high misjudgment may be that the current characteristic parameters are not enough and the personal driving style may have an impact on it. In order to improve the recognition accuracy, we will further analyze the data characteristics under different driving states and

Table 2 The test results of the recognition model

The drivers' actual state	The recognition results of model		Total	Accuracy (%)
	Fatigue	Normal		
Fatigue	163	22	185	83.29
Normal	37	131	168	

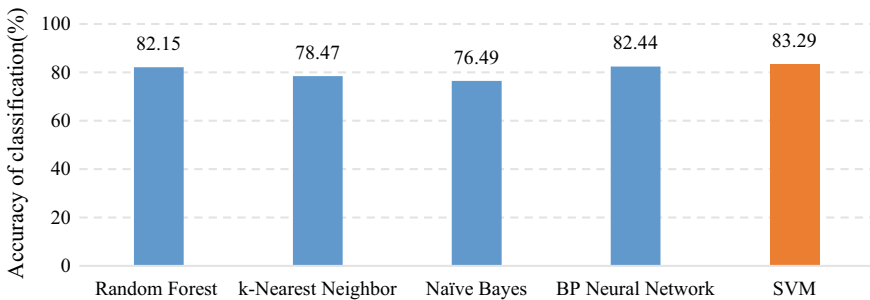


Fig. 11 Performance comparison for different methods

combine with other recognition methods. For the impact of driving style, we will also consider building personalized recognition model of fatigue driving by using smart watch in the following study.

5 Conclusion

The steering operation of a driver under fatigue and normal states will be different. This paper designs and implements a recognition method of fatigue driving based on steering operation by using wearable smart watch. In this proposed method, thirteen principal characteristic parameters are selected from smart watch's sensors by using PCA, and fatigue driving recognition model is established based on SVM. The test results prove that we can use smart watch to recognize the drivers' fatigue or normal state effectively. We also compare the used model in this paper to the other related models. Consequently, the classification accuracy of SVM is better than the other models. This method uses no other external sensors, is low cost, user-friendly and simple. We will further consider more characteristics and build personalized recognition model by using smart watch to improve the accuracy.

Acknowledgements This work was supported by the National Natural Science Foundation of China (Grant No. 61573075), the National Key R&D Program (Grant No. 2016YFB0100904), the Natural Science Foundation of Chongqing (Grant No. cstc2017jcyjBX0001).

References

1. Khushaba RN, Kodagoda S, Lal S et al (2010) Driver drowsiness classification using fuzzy wavelet-packet-based feature-extraction algorithm. *IEEE Trans Biomed Eng* 58(1):121–131
2. Filtness AJ, Anund A, Fors C et al (2014) Sleep-related eye symptoms and their potential for identifying driver sleepiness. *J Sleep Res* 23(5):568–575
3. Mandal B, Li L, Wang GS et al (2017) Towards detection of bus driver fatigue based on robust visual analysis of eye state. *IEEE Trans Intell Transp Syst* 18(3):545–557
4. Wang H, Zhang C, Shi T et al (2015) Real-time EEG-based detection of fatigue driving danger for accident prediction. *Int J Neural Syst* 25(2):1550002
5. Chui KT, Tsang KF, Chi HR et al (2016) An accurate ECG-based transportation safety drowsiness detection scheme. *IEEE Trans Ind Inf* 12(4):1438–1452
6. Chang TH, Hsu CS, Wang C et al (2008) Onboard measurement and warning module for irregular vehicle behavior. *IEEE Trans Intell Transp Syst* 9(3):501–513
7. Zhang X, Cheng B, Feng R (2010) Real-time detection of driver drowsiness based on steering performance. *J Tsinghua Univ* 50(7):1072–1076
8. Kaplan S, Guvensan MA, Yavuz AG et al (2015) Driver behavior analysis for safe driving: a survey. *IEEE Trans Intell Transp Syst* 16(6):3017–3032
9. Wei LI, Chang HQ, Min FX (2010) Detection of driver's fatigue based on vehicle performance output. *J Shanghai Jiaotong Univ* 44(2):292–296
10. Mcdonald AD, Lee JD, Schwarz C et al (2014) Steering in a random forest: ensemble learning for detecting drowsiness-related lane departures. *Hum Factors* 56(5):986–998

11. Mannini A, Sabatini AM, Intille SS (2013) Human gait detection from wrist-worn accelerometer data. *Gait Posture* 37(1):26–27
12. Shoaib M, Bosch S, Incel OD et al (2016) Complex human activity recognition using smartphone and wrist-worn motion sensors. *Sensors* 16(4):426
13. Akerstedt T, Gillberg M (1990) Subjective and objective sleepiness in the active individual. *Int J Neurosci* 52(1–2):29–37
14. Chuan XU, Wang X, Chen X et al (2015) Driver drowsiness level analysis and predication based on decision tree. *J Tongji Univ* 43(1):75–81
15. Cortes C, Vapnik V (1995) Support-vector networks. *Mach Learn* 20(3):273–297